

Numerical homogenization for wave propagation in fractured media

Cite as: AIP Conference Proceedings 2025, 100002 (2018); <https://doi.org/10.1063/1.5064931>
Published Online: 25 October 2018

U. Gavrilieva, V. Alekseev, and M. Vasilyeva



View Online



Export Citation

ARTICLES YOU MAY BE INTERESTED IN

[Numerical simulation of the transport and flow problems in perforated domains using generalized multiscale finite element method](#)

AIP Conference Proceedings 2025, 100001 (2018); <https://doi.org/10.1063/1.5064930>

[Mathematical modeling of the fluid flow and geo-mechanics in the fractured porous media using generalized multiscale finite element method](#)

AIP Conference Proceedings 2025, 100009 (2018); <https://doi.org/10.1063/1.5064938>

[Multiscale model reduction of the flow problem in fractured porous media using mixed generalized multiscale finite element method](#)

AIP Conference Proceedings 2025, 100008 (2018); <https://doi.org/10.1063/1.5064937>



Your Qubits. Measured.

Meet the next generation of quantum analyzers

- Readout for up to 64 qubits
- Operation at up to 8.5 GHz, mixer-calibration-free
- Signal optimization with minimal latency

Find out more



Numerical Homogenization for Wave Propagation in Fractured Media

U. Gavrilieva^{1,a)}, V. Alekseev¹ and M. Vasilyeva^{1,2}

¹*Multiscale model reduction Laboratory, North-Eastern Federal University, Yakutsk, Russia*

²*Institute for Scientific Computation, Texas A&M University, College Station, TX, USA*

^{a)}Corresponding author: lanasemna@mail.ru

Abstract. In this work, we consider a homogenization methods to solve the Helmholtz problem related to elastic wave propagation in fractured media in the frequency domain. We solve local problems for calculation of the effective elastic properties and use them for coarse grid approximation. In the local problems, we use a symmetric interior penalty discontinuous Galerkin (IPDG) method with linear-slip model to represent the fractures. The results of the numerical solution for the two-dimensional problem are presented for model problems.

INTRODUCTION

Wave propagation through fractured porous media plays an important role in seismology. Knowledge of the orientation and spatial distribution of fractures in rocks is highly important in simulations. For small scale fractures whose sizes are much smaller than the seismic wavelength, the effective medium approach can be applied and leads to seismic anisotropy [1, 2, 3].

Numerical simulation of the wave equation in the fractured media is complex problem because there is a need to resolve the wavelength and fracture distribution by mesh. This leads to the problems with a very large dimension and high computational complexity. For numerical solution of the such problems multiscale methods or homogenization techniques are usually used [4].

The effects of fractures on the seismic propagation can be obtained by writing the effective properties as the sum of the compliance tensor of the unfractured background rock and the compliance tensors for each set of parallel fractures or aligned fractures. When considering multidimensional wave equations in fractured media, it is necessary to use numerical methods to capture complex fracture distribution. The numerical homogenization procedure is based on the corresponding discretization techniques and solves local problems that are further coupled in the global formulation.

In this paper, we consider the numerical homogenization to solve the Helmholtz problem related to elastic wave propagation in fractured media in the frequency domain. The obtained effective coefficients are used to solve the complete problem on a coarse grid. The numerical implementation of the problem is based on the finite element approximation using the FEniCS computational platform [5]. We present numerical results and effective elasticity tensors from the analytical formula and for numerical homogenization method. We consider several two-dimensional test cases with different fracture orientation.

PROBLEM FORMULATION AND FINITE ELEMENTS APPROXIMATION

We consider the Helmholtz equation for the elastic waves propagation in the computational domain Ω [1, 2]

$$-\operatorname{div} \sigma - \omega^2 \rho u = f, \quad x \in \Omega \quad (1)$$

where ω is frequency, ρ is density, f is the source function and $u = Re(u) + iIm(u)$. For the stress-strain relation, we have

$$\sigma(u) = C : \varepsilon(u),$$

where C is the coefficients of the elasticity tensor.

In the computations, the energy of waves needs to be absorbed at artificial boundaries in order to avoid spurious reflections caused by the finite computational domain [12]. We use a first order absorbing boundary condition

$$i\rho\omega Au = -\sigma(u)n, \quad x \in \partial\Omega. \quad (2)$$

For numerical solution, we use a finite element method. The weak formulation of the Helmholtz equation for the classical continuous Galerkin method is given by

$$\int_{\Omega} (\sigma(u), \varepsilon(v)) dx - \int_{\Omega} \rho\omega^2 uv dx = \int_{\Omega} f v dx, \quad (3)$$

where $u = \sum_j u_j \phi_j$, ϕ_j are linear basis functions for the fine scale approximation.

ANALYTICAL EFFECTIVE MEDIA PROPERTIES

The effective compliance tensor of the fractured rock can be written as the sum of the compliance tensor of the background medium and that of each set of fractures [9]. The stiffness tensor is obtained by inversion of the compliance tensor.

For the stress-strain relations for the background medium, we have $\sigma = C : \varepsilon$ and $\varepsilon = S : \sigma$, where C and S are the coefficients of the elasticity and compliance tensor of the unfractured background rock.

For a fractured medium, the compliance matrix can be written as

$$\varepsilon_{ij} = S_{ijkl}^* \sigma_{kl}, \quad S^* = S + \sum_{i=1}^{N_f} S^{f,i}, \quad (4)$$

where N_f the number of fracture sets and possible effects of any fracture intersections can be neglected [11]. Here $S^{f,i}$ is the fracture compliance tensor of the i th set of fractures, S is the compliance tensor of the unfractured host medium, and S^* is the compliance matrix of the equivalent medium.

In the long-wavelength limit, *i.e.*, when the applied stress is assumed to be constant over the representative volume, we have the following fracture compliance matrix

$$S^{f,i} = \begin{bmatrix} S_{11}^{f,i} & S_{12}^{f,i} & S_{13}^{f,i} \\ S_{12}^{f,i} & S_{22}^{f,i} & S_{23}^{f,i} \\ S_{13}^{f,i} & S_{23}^{f,i} & S_{33}^{f,i} \end{bmatrix} \quad (5)$$

where

$$\begin{aligned} S_{11}^{f,i} &= \frac{3z_1^i + z_2^i}{8} + \frac{z_1^i}{2} \cos 2\beta^i + \frac{z_1^i - z_2^i}{8} \cos 4\beta^i, & S_{12}^{f,i} &= \frac{z_1^i - z_2^i}{8} (1 - \cos 4\beta^i), \\ S_{22}^{f,i} &= \frac{3z_1^i + z_2^i}{8} - \frac{z_1^i}{2} \cos 2\beta^i + \frac{z_1^i - z_2^i}{8} \cos 4\beta^i, \\ S_{13}^{f,i} &= \frac{z_1^i}{2} \sin 2\beta^i + \frac{z_1^i - z_2^i}{4} \sin 4\beta^i, & S_{33}^{f,i} &= \frac{z_1^i + z_2^i}{2} - \frac{z_1^i - z_2^i}{2} \cos 4\beta^i, \\ S_{23}^{f,i} &= \frac{z_1^i}{2} \sin 2\beta^i - \frac{z_1^i - z_2^i}{4} \sin 4\beta^i, \end{aligned}$$

where the i th set of fractures makes an angle β^i with respect to the x_2 axis [9].

Then, for the elasticity matrix of the equivalent medium, we have

$$C^* = [S + \sum_i S^{f,i}]^{-1} = [C^{-1} + \sum_i S^{f,i}]^{-1}. \quad (6)$$

After calculation of the effective medium properties, we solve the Helmholtz equation with effective elasticity matrix C^* . This technique is widely used for the calculation of the anisotropic effective medium properties and is similar to the harmonic average of the coefficients. Another way for calculation of the effective properties is using homogenization methods by solution of the local problem.

NUMERICAL CALCULATION OF THE EFFECTIVE PROPERTIES

The main idea of numerical homogenization is to identify effective coefficients in coarse cell, C^* . The fractures are captured in the effective elasticity tensor and calculated by solution of the local problem in the representative volume

$$-\operatorname{div} \sigma(u) = 0, \quad x \in K, \quad (7)$$

with Dirichlet boundary conditions

$$u^{(rs)} = \Lambda^{(rs)} x \quad \text{on } \partial K. \quad (8)$$

where

$$\Lambda_{ij}^{(rs)} = \frac{1}{2} (\delta_{ir} \delta_{js} + \delta_{is} \delta_{jr}), \quad r, s = 1, 2. \quad (9)$$

Fractures are modeled by an interface condition, where displacements have discontinuity across a fracture but stress is continuous. These interface conditions (the linear slip interface model, LSM [6]) can describe complex interactions between seismic waves and fractures.

We assume that the fractures have a vanishing width and following the linear-slip model, we have a linear relation between traction vector and the magnitude of the discontinuity in the displacement field as follows

$$[u] = Z \sigma \cdot n, \quad (10)$$

where $[u]$ is the jump of the displacement field at the fracture, $\sigma \cdot n$ is the traction vector at the surface of the fracture and Z is the fracture compliance matrix.

The compliance matrix is diagonal and positive definite, and is given in the 2D case by

$$Z = \begin{bmatrix} z_1 & 0 \\ 0 & z_2 \end{bmatrix}$$

where $z_1 = k_1^{-1}$ and $z_2 = k_2^{-1}$ are the normal and tangential compliances [6, 7, 8].

We use the IPDG method for approximation of the local problem and have following variation formulation: find $u^{(rs)} \in V_h(K)$ such that

$$a_{DG}(u^{(rs)}, v) = 0, \quad v \in V_h(K), \quad (11)$$

and

$$\begin{aligned} a_{DG}(u, v) = & \int_K (\sigma(u), \varepsilon(v)) dx - \int_{\Gamma_0} \{\sigma(u)n\} [v] ds - \int_{\Gamma_0} \{\sigma(v)n\} [u] ds \\ & + \frac{\gamma_f}{h} \int_{\Gamma_0} \{\lambda + 2\mu\} [u][v] ds + \sum_i \int_{\gamma_i} Z^{-1} [u][v] ds, \end{aligned} \quad (12)$$

where $\{\cdot\}$ and $[\cdot]$ are the average and jump of a vector function u and given by

$$\{u\} = \frac{u|_{K^+} + u|_{K^-}}{2}, \quad [u] = u|_{K^+} - u|_{K^-}.$$

The components of the effective elastic moduli C^* are defined by averaging the local strains

$$C_{rspq}^* = \frac{1}{|K|} \int_K C_{ijkl} \varepsilon_{ij}^{(rs)} \varepsilon_{kl}^{(pq)} dx, \quad (13)$$

where $r, s, p, q = 1, 2$ and $\varepsilon^{(rs)} = \varepsilon(u^{(rs)})$ is the deformation field.

There are existed several approaches for the numerical homogenization methods based on the two-scale asymptotic analysis with solution of the local problems in representative volume K with periodic boundary condition, kinematic or static uniform boundary condition (KUBC or SUBC), or mixed boundary condition [13, 14, 15, 16, 17, 4]. This classical homogenization technique follows a standard algorithm for calculation of the effective material properties and is not capable of capturing the behavior away from the low frequency regime [18, 19].

RESULTS

In this section, we compare effective elasticity tensors for an analytical formula (6) and for numerical homogenization using solution of the local problem in the representative volume (13). We consider three different cases with different fracture orientation (see Figure 1, $\beta = \pi/2 + \alpha$) with similar right-hand side f . For numerical simulation, we set $E = 20.0 \cdot 10^9$ [Pa], $\nu = 0.3$, $\rho = 2300$ [kg/m³] and $f_0 = 15$. For fracture compliance, we set $z_j^{-1} = k_j$, $j = 1, 2$ with $k_1 = 9C_{11}$, $k_2 = k_1(1.0 - \eta/2)$, where $\eta = 0.11$. We set the source term $f(x) = G(x)P(\theta)$, where $P(\theta) = (\cos \theta, \sin \theta)$ is the polar angle of the source force vector with $\theta = 0$ and the spatial function $G(x)$ is defined as point source, $G(x) = \delta(x - x_0)$ with $x_0 = (250, 250)$ assigned as the center of the computational domain. This case related to the gas-saturated fractured porous sandstone [9].

Therefore, we have following elasticity matrix for background unfractured medium and fracture compliance tensor

$$C = \begin{bmatrix} C_{1111} & C_{1122} & C_{1112} \\ C_{1122} & C_{2222} & C_{1222} \\ C_{1112} & C_{1222} & C_{1212} \end{bmatrix} = \begin{bmatrix} \lambda + 2\mu & \lambda & 0 \\ \lambda & \lambda + 2\mu & 0 \\ 0 & 0 & 2\mu \end{bmatrix}$$

$$C = \begin{bmatrix} 26.98 & 11.52 & 0 \\ 11.52 & 26.98 & 0 \\ 0 & 0 & 7.683 \end{bmatrix} \cdot 10^9 \quad \text{and} \quad Z = \begin{bmatrix} 0.0041 & 0 \\ 0 & 0.0043 \end{bmatrix} \cdot 10^{-9}.$$

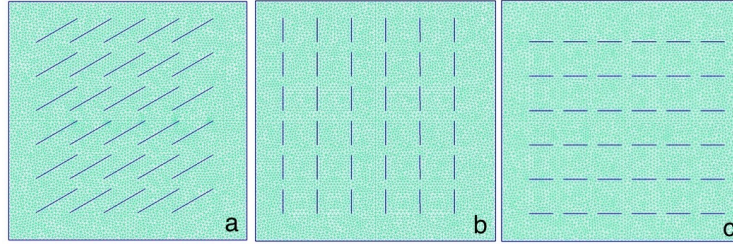


FIGURE 1. Representative volume. Cases a ($\alpha = 30^\circ$), b ($\alpha = 90^\circ$) and c ($\alpha = 0^\circ$)

As an example, at first, we consider a set of vertical and horizontal fractures. For these cases (Case b, c), by (5) we have

$$S^{f,i} = \begin{bmatrix} Z_1 & 0 & 0 \\ 0 & 0 & 0 \\ 0 & 0 & Z_2 \end{bmatrix} \quad \text{and} \quad S^{f,i} = \begin{bmatrix} 0 & 0 & 0 \\ 0 & Z_1 & 0 \\ 0 & 0 & Z_2 \end{bmatrix}, \quad (14)$$

for the vertical and horizontal fractures, respectively. Note that, in the calculation and in domain construction, we use six rows of fracture, $N_f = 6$.

Case with $\alpha = 90^\circ$ (Case b along x_2 direction):

$$C_h^* = \begin{bmatrix} 21.49 & 9.21 & -0.001 \\ 9.21 & 25.90 & -0.002 \\ -0.001 & -0.002 & 7.12 \end{bmatrix} \cdot 10^9$$

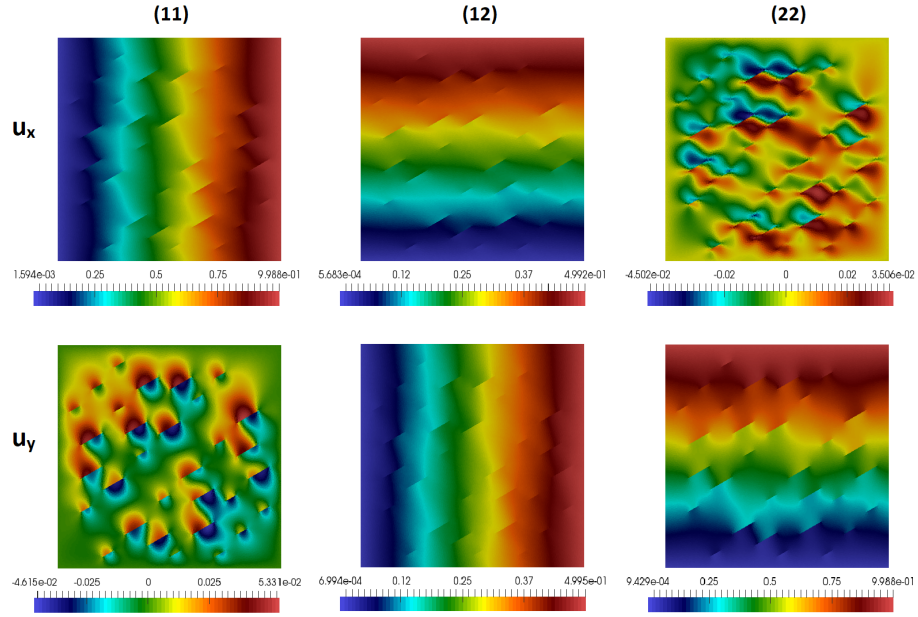


FIGURE 2. Local problem solution in the representative volume (*Case a*)

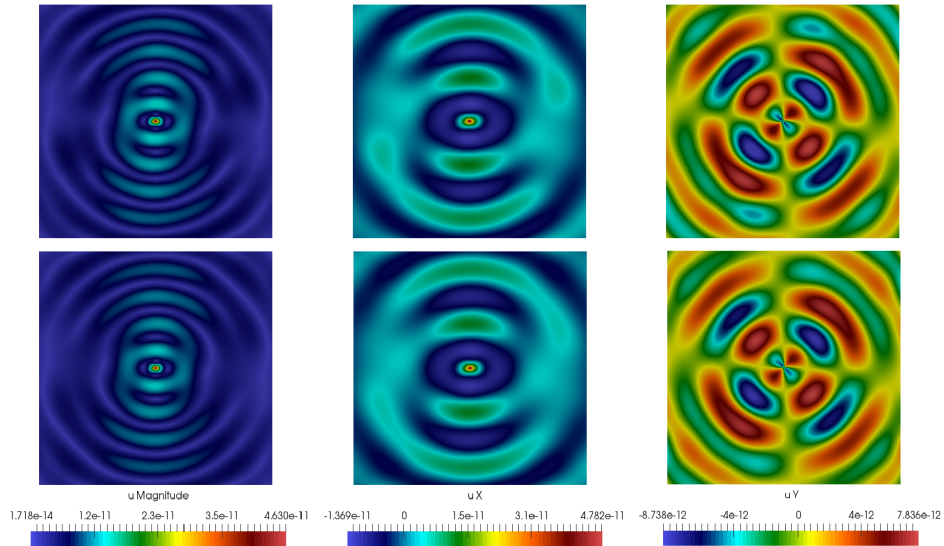


FIGURE 3. Numerical solutions for the domain with $\omega = 2\pi f_0$ and $f_0 = 15$. Displacement magnitude u_m . Top: numerical homogenization for $\alpha = 30^\circ$ (*Case a*). Bottom: analytical formula for $\alpha = 30^\circ$ (*Case a*)

$$C_a^* = \begin{bmatrix} 16.13 & 6.91 & 0 \\ 6.91 & 24.91 & 0 \\ 0 & 0 & 6.39 \end{bmatrix} \cdot 10^9, S^{f,i} = \begin{bmatrix} 0.0041 & 0 & 0 \\ 0 & 0 & 0 \\ 0 & 0 & 0.0043 \end{bmatrix} \cdot 10^{-9}.$$

Case with $\alpha = 0^0$ (Case *c* along x_1 direction):

$$C_h^* = \begin{bmatrix} 25.87 & 9.14 & 0.0003 \\ 9.14 & 21.33 & 0.0007 \\ 0.0003 & 0.0007 & 7.14 \end{bmatrix} \cdot 10^9$$

$$C_a^* = \begin{bmatrix} 24.91 & 6.91 & 0 \\ 6.91 & 16.13 & 0 \\ 0 & 0 & 6.39 \end{bmatrix} \cdot 10^9, S^{f,i} = \begin{bmatrix} 0 & 0 & 0 \\ 0 & 0.0041 & 0 \\ 0 & 0 & 0.0043 \end{bmatrix} \cdot 10^{-9}$$

Next, we consider Cases with $\alpha = 30^0$ (Case *a*). We have

$$C_h^* = \begin{bmatrix} 23.13 & 7.67 & 1.73 \\ 7.67 & 19.26 & 1.55 \\ 1.73 & 1.55 & 6.87 \end{bmatrix} \cdot 10^9$$

$$C_a^* = \begin{bmatrix} 22.41 & 7.22 & 2.07 \\ 7.22 & 18.02 & 1.72 \\ 2.07 & 1.72 & 6.70 \end{bmatrix} \cdot 10^9, S^{f,i} = \begin{bmatrix} 0.0010 & 0 & -0.0018 \\ 0 & 0.0031 & -0.0017 \\ -0.0018 & -0.0017 & 0.0041 \end{bmatrix} \cdot 10^{-9},$$

In Figure 2, we calculate solution of the local problem in the representative volume. In Figure 3, we present real part of solution magnitude for elastic fractured media with anisotropic elasticity matrix for $\alpha = 30^0$ (Case *a*) using different methods for the calculations of the effective medium properties. We can see, how the anisotropic effective stiffness matrix change the shape of the wavefront. We obtain similar behavior for numerical homogenization and for analytical formula. Both effective stiffness matrices are symmetric.

CONCLUSION

We have considered the elastic wave propagation in fractured media in the frequency domain. For numerical solution on a coarse grid, we used a finite element method. The effective elastic properties are calculated by solution of the local problems, where we used a symmetric interior penalty discontinuous Galerkin (IPDG) method for approximation with linear-slip model to represent the fractures. The results of simulation using the developed method are presented for two-dimensional model problems. Our numerical results show a good agreement and show that numerical homogenization techniques can be effectively used for this problem.

ACKNOWLEDGEMENTS

The work is supported by the mega-grant of the Russian Federation Government (No 14.Y26.31.0013).

REFERENCES

- [1] J.D. De Basabe, K.S. Mrinal, and M.F. Wheeler (2011) Seismic wave propagation in fractured media: a discontinuous Galerkin approach, *SEG Expanded Abstr.* **30**.
- [2] J.D. De Basabe, K.S. Mrinal, and M.F. Wheeler (2016) Elastic wave propagation in fractured media using the discontinuous Galerkin method, *Geophysics* **81**(4), T163–T174.
- [3] L.J. Pyrak-Nolte, L.R. Myer, and N.G. Cook (1990) Transmission of seismic waves across single natural fractures, *Journal of Geophysical Research: Solid Earth* **95**(B6), 8617–8638.
- [4] E.T. Chung, Y. Efendiev, R.L. Gibson, and M. Vasilyeva (2016) A generalized multiscale finite element method for elastic wave propagation in fractured media, *GEM-International Journal on Geomathematics* **7**, 163–182.
- [5] Computational platform FEniCS, <https://fenicsproject.org>.
- [6] M. Schoenberg (1980) Elastic wave behavior across linear slip interfaces, *The Journal of the Acoustical Society of America* **68**(5), 1516–1521.
- [7] C.-J. Hsu and M. Schoenberg (1993) Elastic waves through a simulated fractured medium. *Geophysics* **58**(7), 964–977.

- [8] J. Zhang (2005) Elastic wave modeling in fractured media with an explicit approach, *Geophysics* **70**(5), T75–T85.
- [9] M. Schoenberg and C.M. Sayers (1995) Seismic anisotropy of fractured rock, *Geophysics* **60**(1), 204–211.
- [10] M. Schoenberg, S. Dean, and C.M. Sayers (1999) Azimuth-dependent tuning of seismic waves reflected from fractured reservoirs, *Geophysics* **64**(4), 1160–1171.
- [11] D. Nichols, F. Muir, and M. Schoenberg, “Elastic properties of rocks with multiple sets of fractures,” in *SEG Technical Program Expanded Abstracts 1989* (Society of Exploration Geophysicists, 1989), pp. 471–474.
- [12] B. Engquist and A. Majda (1977) Absorbing boundary conditions for numerical simulation of waves, *Proceedings of the National Academy of Sciences USA* **74**(5), 1765–1766.
- [13] Ch. Huet (1990) Application of variational concepts to size effects in elastic heterogeneous bodies, *Journal of the Mechanics and Physics of Solids* **38**(6), 813–841.
- [14] T. Kanit, S. Forest, I. Galliet, V. Mounoury, and D. Jeulin (2003) Determination of the size of the representative volume element for random composites: statistical and numerical approach, *International Journal of Solids and Structures* **40**(13), 3647–3679.
- [15] R. Cottreau (2013) Numerical strategy for unbiased homogenization of random materials, *International Journal for Numerical Methods in Engineering* **95**(1), 71–90.
- [16] S. Hazanov and C. Huet (1994) Order relationships for boundary conditions effect in heterogeneous bodies smaller than the representative volume, *Journal of the Mechanics and Physics of Solids* **42**(12), 1995–2011.
- [17] E. Sánchez-Palencia, Non-homogeneous media and vibration theory, *Lecture Notes in Physics*, vol. 127, 1980.
- [18] R.V. Craster, J. Kaplunov, and A.V. Pichugin (2010) High-frequency homogenization for periodic media, *Proceedings of the Royal Society of London A: Mathematical, Physical and Engineering Sciences* **466**, 2341–2362.
- [19] L.F. Fan, G.W. Ma, and L. Ngai Yuen Wong (2012) Effective viscoelastic behaviour of rock mass with double-scale discontinuities, *Geophysical Journal International* **191**(1), 147–154.